Study on Crosstalk Reduction in Resonant-Cavity-Enhanced PD-Array for WDM-beam direct detection

Riki Ishizawa
Department of Electronic and Physical Systems, School of Fundamental Science and Engineering,
Waseda University
Tokyo, Japan
riki.i.0407.gcs8@akane.waseda.jp

Shoichi Takamizawa
Fuji Research Corporation
Kanagawa, Japan
sho_takamizawa@ftr.co.jp

Toshimasa Umezawa
Optical Access Technology Laboratory
Photonic ICT Research Center
Network System Research Institute
Tokyo, Japan
toshi_umezawa@nict.go.jp

Naokatsu Yamamoto
Photonic ICT Research Center
Network System Research Institute
Tokyo, Japan
naokatsu@nict.go.jp

Kouichi Akahane
Optical Access Technology Laboratory
Photonic ICT Research Center
Network System Research Institute
Tokyo, Japan
akahane@ nict.go.jp

Tetsuya Kawanishi
Department of Electronic and Physical Systems, School of Fundamental Science and Engineering,
Waseda University
Tokyo, Japan
kawanishi@waseda.jp

***Abstract*—In this study, we present a resonant cavity-enhanced two-dimensional-photodetector (PD) array device, which can receive four different wavelengths simultaneously in free space. A different wavelength sensitivity in each resonant PD pixel allows de-multiplexing wavelength in wavelength division multiplexing (WDM) beam signal in free space. We discuss the crosstalk reduction design in the PD array for 4-WDM FSO beam direct detection and its fabricated device performance.**

Keywords—Resonant-cavity-enhanced photodetector, WDM, crosstalk

I. INTRODUCTION

The transmission capacity of single-mode fiber (SMF), which is commonly used today, is approaching its limit, and problems are expected to become apparent soon [1]. To increase the data rate per line or per wavelength, multiplexing technologies such as multilevel modulation format technology, wavelength division multiplexing (WDM) and space division multiplexing (SDM) technology have attracted attention to overcome the transmission capacity limitation of SMF.

Moreover, free space optical (FSO) communication is one of good candidates for advanced wireless communications in beyond-5G, which can achieve a high data rate and fiber communications. WDM technology with OOK modulation format has been mainly studied to increase the data rate [2]. In the FSO system, a small footprint in compact FSO transmitter-receiver is required by using integrated high-speed photonic devices. In contrast, we reported an integrated high-speed photodetector array device [3] that consists of a two-dimensional (2D) aligned arrangement design for advanced fiber and FSO communications. The integrated 2D-PD array device enables not only enlarging optical alignment tolerance, but also increasing signal-to-noise ratio with digital signal processing using multi-output signals from PD arrays (Fig. 1).

In this study, we present a resonant cavity-enhanced 2D-photodetector array device applied from our previous works. A different wavelength sensitivity in each resonant PD pixel allows a de-multiplexing wavelength in WDM beam signal in free space. The crosstalk reduction design in PD array for directly detecting 4-WDM FSO beam and its fabricated device performance are discussed.

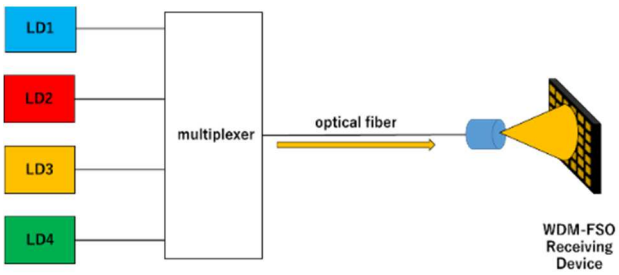

Fig. 1 Schematic view graph of WDM-FSO transmission system using integrated 2D-PD array

II. CROSSTALK ANALYSIS

Firstly, we experimentally evaluated bit error rate (BER) in relation to crosstalk between two optical signals (10 Gbps, OOK) with different wavelengths, assuming 2-WDM signal detection by a PD array device. Fig. 2 shows the experimental setup used for the evaluation. The experimental flow is as follows: First, we adopted 1550 nm and 1555 nm two DFB lasers, and then were modulated by using a Lithium Niobate (LN) modulator and a bit pattern generator. An attenuator (ATT) was then used to fix the power of the 1550 nm signal at -8.3 dBm and vary the power of the 1555 nm signal from -18.3 dBm to -7.8 dBm. The coupling of the two light waves was performed using an optical coupler, and the spectrum at that time was observed using a spectrum analyzer. In this experiment, representative spectra at 1550 nm and 1555 nm are shown in Fig. 3. The signal was received by a commercially available PD (wavelength range of sensitivity: 1300 nm–1600 nm), which can detect those two signals simultaneously, and the waveform was observed using an oscilloscope. Finally, the communication quality was examined using a BER tester.

The measurement result on BER when the power of the 1550 nm signal was fixed at -8.3 dBm and the power of the 1555 nm signal was varied from -18.3 dBm to -7.8dBm is shown in Fig. 4. When the 1550 nm signal light power is larger

than that in the 1555 nm adjacent signal light, a lower BER could be obtained. In particular, when the crosstalk is observed below -6 dB, a good BER of less than 1.0×10^{-9} could be revealed and then high communication quality could be expected. Here, a crosstalk of -6 dB based on the optical power unit corresponds to -12 dB in the photocurrent unit. Therefore, the crosstalk less than -12 dB would be a target value for 2-WDM beam direct detection using the PD array device in this study.

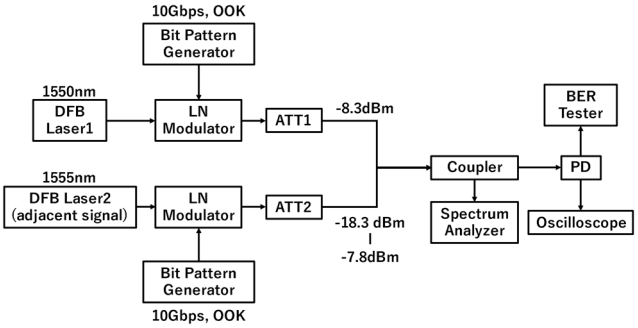

Fig. 2 Experimental setup for bit error rate relation to crosstalk

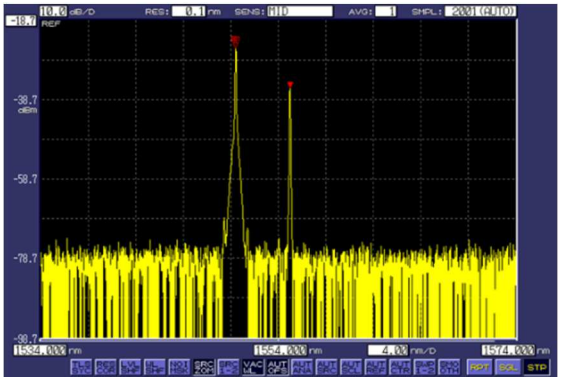

Fig. 3 Spectrum of the 1550 nm signal and the 1555 nm adjacent signal

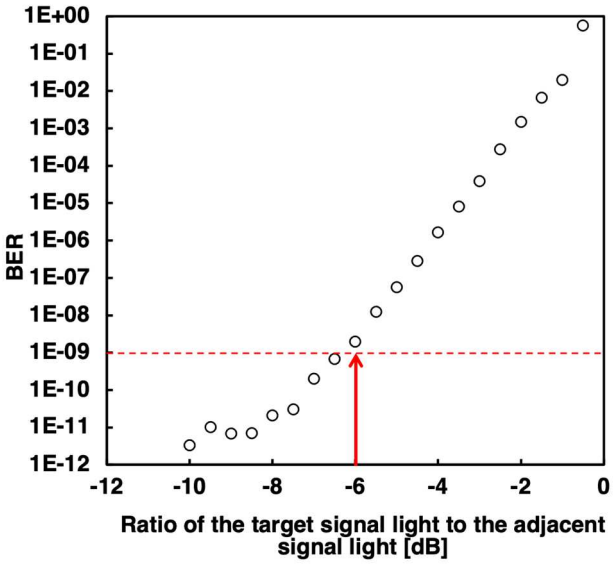

Fig.4 Estimated BER vs crosstalk in two signals

III. Design of RCE-PD array

During the designing of the device structure, we focused on two targets: First, to receive four wavelengths at a pitch of 10 nm (less than 20 nm) referring to the CWDM system; second, the crosstalk of photocurrent quantum efficiency should be less than -12 dB for the crosstalk of light power to be less than -6 dB. Based on these two goals, we performed simulations and determined the structure of the device according to the equation (1)[4].

$$\eta = \frac{(1 + R_2 e^{-\alpha d})(1 - R_1)(1 - e^{-\alpha d})}{1 - 2\sqrt{R_1 R_2} e^{-\alpha d} \cos(2\beta L + \varphi_1 + \varphi_2) + R_1 R_2 e^{-2\alpha d}} \quad (1)$$

Equation (1) is the formula for the quantum efficiency of the RCE-PD. The thickness of the light-absorbing layer is denoted by d; the optical absorption coefficient of the active layer is denoted by α; and φ_1 and φ_2 are the phase shifts that occur when light is reflected by the front and end mirrors. The reflectance of the front and end mirrors are R_1 and R_2, the propagation constant is β, and the distance between the two mirrors is L.

Using equation (1), we performed simulations, and quantum efficiency is obtained, as shown in Fig. 5, when d = 100 nm, R_1 = 80%, R_2 = 95%, and the four cavity lengths were L = 3850 nm, 3900 nm, 3950 nm, and 4000 nm. Furthermore, we calculated the crosstalk as follows:

A. $20 \log\left(\frac{PD1}{PD2}\right) = -27.42[dB]$

B. $20 \log\left(\frac{PD2}{PD1}\right) = -26.49[dB]$

C. $20 \log\left(\frac{PD2}{PD1+PD3+PD4}\right) = -19.63[dB]$

A and B in above are the estimated crosstalk for 2-WDM-RCE-PD consisting of only PD1 and PD2, and C is the crosstalk for 4-WDM-RCE-PD consisting of PD1, PD2, PD3, and PD4. From these calculations, we concluded that the crosstalk could be sufficiently small if the parameters were set to the above values. We determined the structure of the device (Fig. 6) as follows, referring to the parameters obtained in equation (1). First, a distributed bragg reflector (DBR) with muti-stacked alternating layers of InGaAlAs and InP was fabricated on an InP substrate. The DBR had a reflectivity of approximately 95% in the 1500 nm–1600 nm. An i-InGaAs layer with a thickness of 100 nm was sandwiched by un-InP layers with a thickness of 400 nm, and the un-InP layer was sandwiched by thick p-InP and n-InP layers. The HR films were fabricated on the surface of the device using SiO_2 and Si. This HR film has a reflectivity of approximately 80% in the range of 1500 nm–1600 nm. The HR film, DBR, and i-InGaAs layer function acted as the front mirror, the end mirror, and the optical absorption layer, respectively. The un-InP layers sandwiching the optical absorption layer are undoped, which improve frequency characteristics by reducing electrical capacitance.

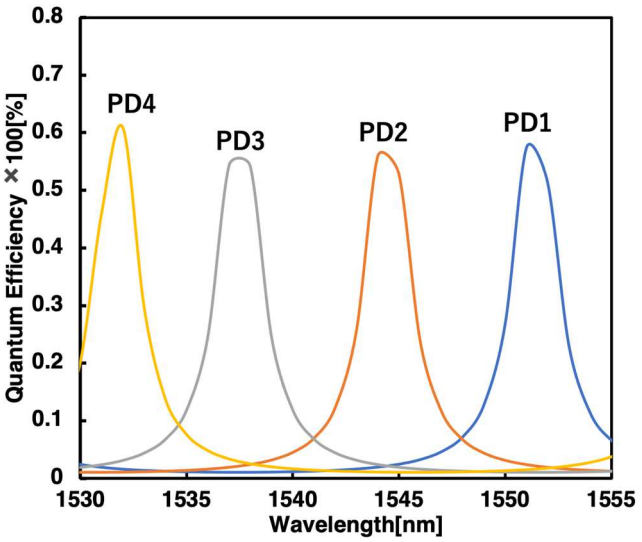

Fig5. Simulated crosstalk of the quantum efficiency for 4-WDM

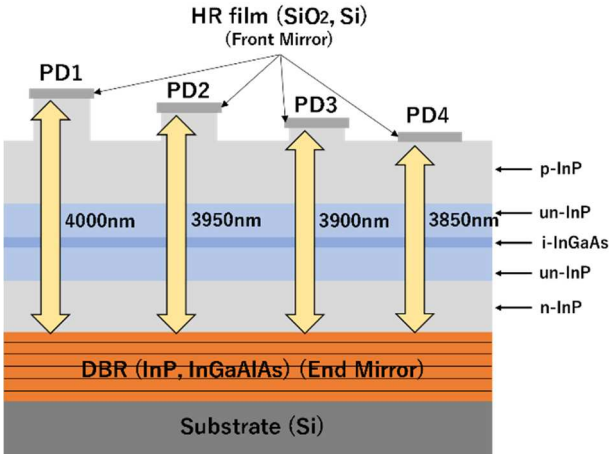

Fig.6 Device structure of the 4-WDM-RCE-PD device

IV. FABRICATION

The fabrication process of the device is illustrated below. We first fabricated the P electrode of PD1. A thin film of Ti, Pt, and Au was formed on epitaxial wafers using an electron beam deposition system. The P electrode of PD1 was completed by removing the unnecessary metal film using the lift-off method. After protecting PD1 with a photoresist to prevent wet etching damage, wet etching of PD2 was performed and adjusted to a cavity length of 3950 nm (PD2). A SiO_2 film was formed over the entire top surface of the wafer using a chemical vapor deposition system. A SiO_2 dry-etching mask was fabricated by a photo-lithography process and buffered hydrofluoric acid (BHF). After the BHF etching was completed, dry-etching was performed down to the middle of the n-InP layer using Cl-based dry etching system. In addition, focus is essential to the etching rate because the pin structure will break if the n-InP layer is over-etched. After removing SiO_2, the N electrode was fabricated on the n-InP layer. The P electrode for PD2 was fabricated using the same procedure as for PD1. Finally, the HR film, which is the front mirror, was fabricated after protecting the electrodes with a photoresist. The device's appearance after the electrodes were fabricated is shown in Fig. 7.

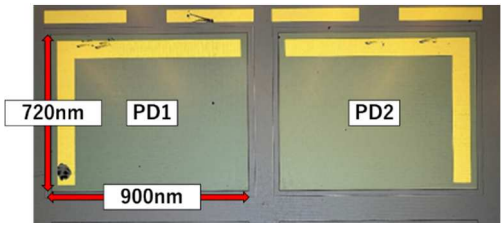

Fig.7 Photograph of fabricated RCE-PD with different cavity length (PD1 = 4000 nm, PD2 = 3950 nm)

V. RESULT

We measured the spectral responsivity characteristics of PD1 and PD2 and calculated their quantum efficiencies. In this experiment, we first applied a bias voltage of 3 V to the device using a DC power supply. We then irradiated the device with laser light using a conventional laser source with an optical power of 0 dBm. We recorded the value of the photocurrent measured using a digital multimeter. The quantum efficiencies of PD1 and PD2 are shown in Fig. 8. It shows that the crosstalk of quantum efficiencies between PD1 and PD2 are -25.57 dB and -26.93 dB, respectively. Because these values are significantly less than -12 dB, high-quality communications with a BER of less than 1.0×10^{-9} can be achieved if 2-WDM communications are performed using this device.

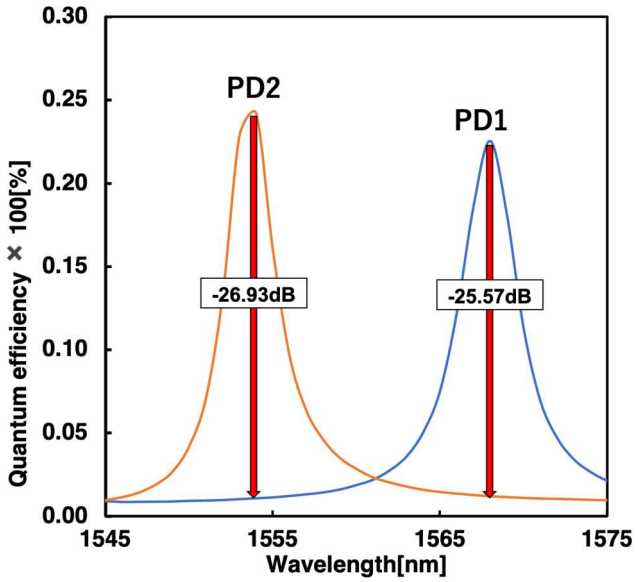

Fig.8 Measurement result on crosstalk between PD1 and PD2

VI. DISCUSSION

First, we compared the calculated crosstalk with the experimental results in PD1 and PD2. As summarized in Table 1, the crosstalk value between the calculated and experimental results is consistent. In addition, because the crosstalk is well below the design target of -12 dB, it is possible to achieve high-quality communication without any problems. Moreover, Table 1 shows that the resonance wavelengths of both PD1 and PD2 are shifted to the longer wavelength. This is supposed to be owing to the longer cavity length than the designed value because of wafer manufacturing errors or uneven etching in

the wet etching process. For the maximum quantum efficiencies of PD1 and PD2, we established a difference between experimental and simulation results for PD1 (calculation = 57.3%, experiment = 22.6%) and PD2 (calculation = 52.7%, experiment = 24.2%). This could be owing to the reflectance of the front and end mirrors. In the simulation, the reflectance of the front mirror was calculated as 80%, and that of the end mirror was 95%; however, the reflectance of each mirror in the fabricated device might be approximately 10% lower than the target value owing to manufacturing errors.

Table 1 Comparison of calculated and experimental results for PD1 and PD2

		Calculated value	Experimental value
Resonance wavelength [nm]	PD1	1551	1568
	PD2	1544	1554
Maximum quantum efficiency [%]	PD1	57.3	22.6
	PD2	52.7	24.2
Crosstalk [dB]	PD1	-26.49	-26.93
	PD2	-27.42	-25.57

Next, we investigated crosstalk experimentally under higher WDM density conditions, where the peak pitch of 10 nm was improved to 5 nm. We fabricated an additional PD (PD5) with a cavity length shorter than that of PD4 (3850 nm), whose quantum efficiency peak position should be located between the peaks of PD1 and PD2. The measurement result on the quantum efficiency for the 3-WDM-RCE-PD are presented in Fig. 9. We successfully achieved low crosstalk in between -13.85 dB and -18.22 dB even when PD5 was considered. Therefore, even under the severe conditions, where the resonance peak of PD5 is between PD1 and PD2 (peak pitch of 5 nm for higher WDM condition), the fabricated device can achieve below -12 dB.

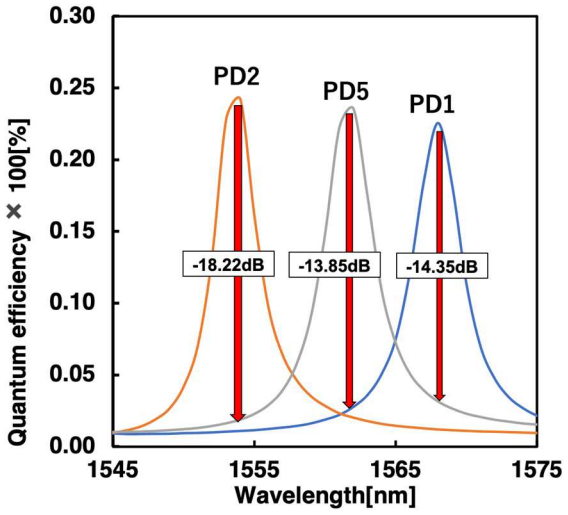

Fig.9 Measurement result on crosstalk among PD1, PD2, and PD5

VII. Conclusion

Herein, we designed a 4-WDM-RCE-PD with a resonance wavelength spacing of 10 nm and a crosstalk of quantum efficiency below -12 dB. To confirm the proof of our design concept, we fabricated and measured the spectral sensitivity and calculated the quantum efficiency in the 2-WDM-PCE-PD and 3-WDM-RCE-PD; the crosstalk was less than -12 dB. Therefore, we can expect a BER less than 1.0×10^{-9} at 10 Gbps and beyond in the 3-WDM beam in the simultaneous direct direction. In the future, we will demonstrate 3-WDM-FSO communication using a downsized pixel-based high-speed RCE-PD array device.

Acknowledgment

This paper includes research results supported by Waseda Research Institute for Science and Engineering. And this research was conducted in part under the contract “R&D of high-speed THz communication based on radio and optical direct conversion” (JPJ000254) in conjunction with the Ministry of Internal Affairs and Communications of Japan. We wish to express our deepest gratitude to the people at the Photonic Device Laboratory of the National Institute of Information and Communications Technology (NICT) for their assistance in using their experimental facilities to conduct this research.

References

[1] K. Saito, et. al., “Increasing the Capacity of Optical Communications with Optical Fiber for Space Division Multiplexing Transmission,” Communications Society Magazine No. 51, pp. 166-176, Winter 2019.

[2] S. Chandra, et. al., “Hybrid WDM-FSO system with spatial multiplexing for 5G Wireless Network using in the presence of Wireless and Optical Nonlinearities,” 2017 14th IEEE India Council International Conference (INDICON), pp.1-6, 2017.

[3] K. Kusakata, et. al., “Characterization of 2D High-speed Photodetector Array Device for SDM Fiber Communication Applications,” 2019 24th OptoElectronics and Communications Conference (OECC) and 2019 International Conference on Photonics in Switching and Computing (PSC), pp.1-3, 2019.

[4] K. Lai, et. al., “Design of a Tunable GaAs/AlGaAs Multiple-Quantum-Well Resonant-Cavity Photodetector,” IEEE Journal of Quantum Electronics, Vol.30 (1), pp.108-114, 1994.